JOURNAL OF MATERIALS SCIENCE **40** (2005) 4767–4774

Phase transformations associated with micropitting in rolling/sliding contacts

A. OILA*, S. J. BULL
School of Chemical Engineering and Advanced Materials, University of Newcastle, Newcastle upon Tyne, NE1 7RU, UK
E-mail: Adrian.Oila@ncl.ac.uk

Published online: 08 July 2005

Metallographic investigation of the discs used in tests to simulate gear tooth contact has revealed the occurrence of several microstructural features that are present only in fatigued specimens: e.g. dark etching regions (DER) and white etching bands (WEB). In addition, a new type of microstructural constituent has been observed close to the surface, below asperities. This feature is referred to as the plastic deformation region (PDR). For the first time the hardness of these fatigue-induced phases was accurately determined by the nanoindentation technique. It has been found that DER initiates at the prior austenite grain boundaries. Fatigue cracks initiate and propagate preferentially at the boundaries of PDR and ultimately lead to the formation of micropitting.

1. Introduction

Peculiar microstructural features have been long reported to occur in pure rolling contacts. As early as in 1946 Jones [1] reported a phenomenon of martensite decay in fatigued ball bearings. He observed a dark etching region beneath the ball track of bearing inner races and claimed the occurrence of pitting as a consequence. This was attributed to a tempering phenomenon caused by the heat generated within the contact and the new phase was called troostite. Since then the decay of martensite has been thoroughly investigated [2–22] and an adequate terminology has been adopted [10]. Due to their etching characteristics, the products of martensite decay are called: dark etching regions (DER) and white etching bands (WEB). DER represents a mixture of residual martensite with a ferritic phase that contains carbon in excess (corresponding to that in martensite) which is inhomogeneously distributed [10, 17]. WEB have the appearance of thin elongated stringers and they are lightly etched by nital [3, 8]. There are two sets of WEB. The first set consists of disc-shaped regions of ferrite inclined at 30° to the surface in the direction opposite to that of rolling, bordered by carbide discs which are constituted of very small carbide particles [10, 15] with 15–30 at.% carbon [15]. The second set of WEB are disc-shaped regions of plastically deformed ferrite inclined at 80°t o the surface [10]. TEM investigations [10, 13] showed that the 80°-WEB has a fine cell structure resembling heavily deformed ferrite and is free of carbides [3, 5, 12]. Sometimes the white etching bands were confused with the white etching wings of the butterflies first described by Styri in 1951 [23]. A butterfly is a double wing-like region, associated with non-metallic inclusions or carbides, which is light etched compared to the martensite matrix. The mechanism of their formation depends on the recrystallisation of ferrite grains which undergo work hardening under cyclic stressing [24]. It was found by TEM investigation [12] that DER and butterfly wings have the same microstructure which implies that both transformations are different manifestations of the same mechanism.

A point of confusion relates to the microhardness of the decayed martensite. It was reported that DER is harder than the martensite matrix by some authors [19] while most others reported to be softer [2, 10, 17]. Most authors reported that the butterfly's wing hardness is higher [4, 24] than the martensite matrix while the DER hardness is lower [2, 10, 17] which is confusing since both phases have similar microstructure. It appears that conventional microhardness testing is not the appropriate method for such fine and inhomogeneous microstructure and only nanoindentation can give reliable results.

The microstructural changes described above are responsible for fatigue failure of bearings [25, 26]. There are only a few cases in which martensite decay has been reported in rolling/sliding contacts. However it is not clear if and how this contributes to the damage of the gear tooth flank. Hoeprich [27] believes that the dark etching effect in gears is due to plastic deformation and dislocation accumulation rather than phase transformation or that it is due to the diffusion of hydrogen

*Author to whom all correspondence should be addressed.
0022–2461
DOI: 10.1007/s10853-005-2017-5

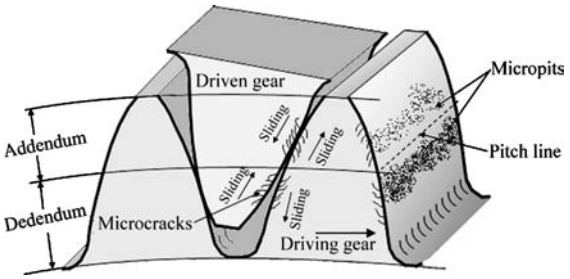

Figure 1 Schematic drawing showing micropits and microcracks in gear tooth.

from the lubricant to the steel as a result of tribological processes in asperity contacts. White etching areas (but not bands) have been described by Winter *et al.* [28] but they assume they do not cause fatigue damage on tooth flanks. Some of these white etching areas (WEA) form around inclusions and they would probably be better described as butterflies. It has been shown recently [29] that the decay of martensite also occurs in specimens subjected to rolling/sliding loading, both discs and gears.

Micropitting is a form of surface contact fatigue encountered in bearings and gears, under lubricating conditions, which lead to their premature failure. Microscopically, micropitting shows similar features (i.e. pits and cracks, see Fig. 1) as macropitting but these differ in scale. A micropit is characterised by a depth, length and width on the order of a few microns or tens of microns. The microcracks have different orientations in the dedendum and addendum (see Fig. 1), which suggests that their orientation depends on the sliding direction (i.e., the direction of the friction force). On the driving gear (pinion) the cracks propagate towards the pitch line meanwhile on the driven gear (wheel) cracks propagate away from the pitch line. The cracks propagate into the depth of the steel at a shallow angle, usually less than 30°.

All gears are susceptible to micropitting, including spur, helical and bevel. Micropitting can occur with all heat treatments applied to gears and with both, synthetic and mineral lubricants [30]. It can occur after a relatively short period of operation and, in some cases, after less than a million cycles gears need to be replaced due to the increased noise and vibrations caused by the deviation of the tooth profile. Continuing operation of affected gears can lead to a catastrophic type of failure (i.e., tooth breakage [30]).

The purpose of the present work is to present the results of the metallographic investigation carried out on disc specimens tested in conditions similar to those encountered in gear applications. In addition to DER and WEB, zones that exhibit an apparently non-martensitic microstructure have been found near the tested surface. These zones are referred to as plastic deformation regions (PDR). The hardness of these phases have been determined by the nanoindentation technique.

The micropitting mechanisms suggested previously are explained in terms of lubricant pressure effects inside the crack [31] or slip line field theory [32, 33] but with no reference to the steel microstructure. This is addressed in this paper.

TABLE I Chemical composition of the 655H13 steel (wt.%)

C	Mn	Cr	Ni	Si	Mo	S	P
0.12	0.55	1.2	3.25	0.28	0.12	0.025	0.025

2. Experimental

2.1. Sample preparation

The discs were made from 655H13 steel which is widely used for gear manufacturing. The chemical composition of the steel is given in Table I.

After carburising at 925°C for 8 h the samples were quenched in agitated oil and tempered at 150°C for 2 h. The case depth achieved was 1.5 mm. Following heat treatment the discs were first ground on both flat faces and then on the test surface. For studying the influence of surface topography on micropitting the contact surface of the discs was circumferentially and axially ground. Axial grinding produces transverse lay which represents a better simulation of gear contact conditions, considering that, on the gear tooth, the direction of grinding marks and the direction of contact motion are perpendicular. The surface finish achieved was about $R_a = 0.4\ \mu$m which is a common value for gears. The amount of retained austenite determined by XRD technique at the test surface was 15% prior testing and 7% after testing.

2.2. Micropitting test

Experiments made on roller discs faithfully reproduce micropitting as found in gears [29, 34, 35]. In addition, these types of tests are less expensive and the times to failure are considerably shorter. Micropitting experiments were carried out using a two-disc machine designed at the University of Newcastle. A complete description of the rig is given in [29]. Disc samples have an inner diameter of 25 mm to fit on the shafts. The sum of the outer diameters is 120 mm. Different slide-to-roll ratios can be achieved by choosing discs of different diameters but keeping constant the sum of the diameters of the two discs.

Experiments were carried out with two different lubricants, a mineral oil with 4% EP additives (Anglamol A99) and a synthetic oil, OEP-80, used for marine gear lubrication. The test conditions in the micropitting experiments are listed in Table II.

2.3. Metallographic examination

The microstructure has been observed in two locations, by sectioning the disc in longitudinal and transverse direction as shown in Fig. 2. The detail at the edge of the specimen is of the greatest importance in this study. In order to ensure the edge retention during grinding and polishing, the curved surface of the specimens has been

TABLE II Test conditions in the micropitting experiments

Exp.	Surface lay	Contact pressure (MPa)	Lubricant	Temperature (°C)	Speed (rpm)	Slide/roll ratio
1	Longitudinal	1800	Mineral	60	1200	0.33
2	Transverse	2200	Synthetic	100	1200	0.33
3	Longitudinal	2200	Mineral	100	1000	0.23

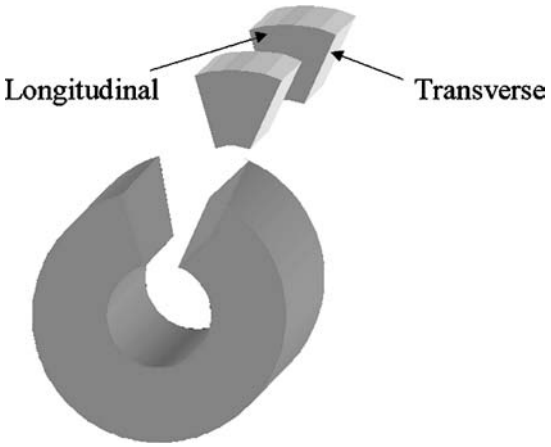

Figure 2 Locations of metallographic investigations: longitudinal and transverse.

nickel plated in a Watts nickel bath. The other sides of the specimens were masked with lacquer. Specimens were mounted in a carbon filled epoxy resin in order to avoid the occurrence of charging during subsequent SEM investigation. Grinding was carried out successively on 240 and 600 SiC papers lubricated by water and then the specimens were polished on alumina cloths of 9, 3 and 1 μm size. In order to reveal the microstructure two types of etchants have been used: nital and picral. DER are only revealed by the nital etch [13] whereas the best resolution for the WEB is achieved by etching with picral solution [3]. Nital etches ferrite grain boundaries and ferrite-cementite grain boundaries, while picral attacks the phase boundary between ferrite and cementite or other carbides but not the boundaries between ferrite grains [36].

2.4. Nanoindentation test

The hardness of different phases present in the gear steel (DER, WEB, and PDR) was determined by the nanoindentation technique using peak load of 10 mN. Hardness was determined by the method of Oliver and Pharr [37] and corrected for the effect of pile-up by calibration factor determined from AFM analysis of the residual impressions using the approach developed previously [38].

3. Results

The microscopic examination of the samples etched with nital has revealed the occurrence of microstructural features similar to those reported in fatigued bearings, i.e. DER and WEB. Fig. 3 shows two cross sections of the disc tested in experiment 1 taken in longitudinal direction in (b) and transverse direction in (c). DER are clearly seen in both pictures, beneath the specimen surface. These regions appear much darker than the rest of the microstructure. Beneath the dark etching zone, the microstructure is characterised by a preferential oriented texture (see Fig. 3b). The texture consists of white lines (WEB), which lie between 185 and 690 μm below the contact surface. In Fig. 3b WEB are inclined to the surface plane to an angle $\alpha = 45^\circ$ in the direction opposite to the sliding direction. WEB are not

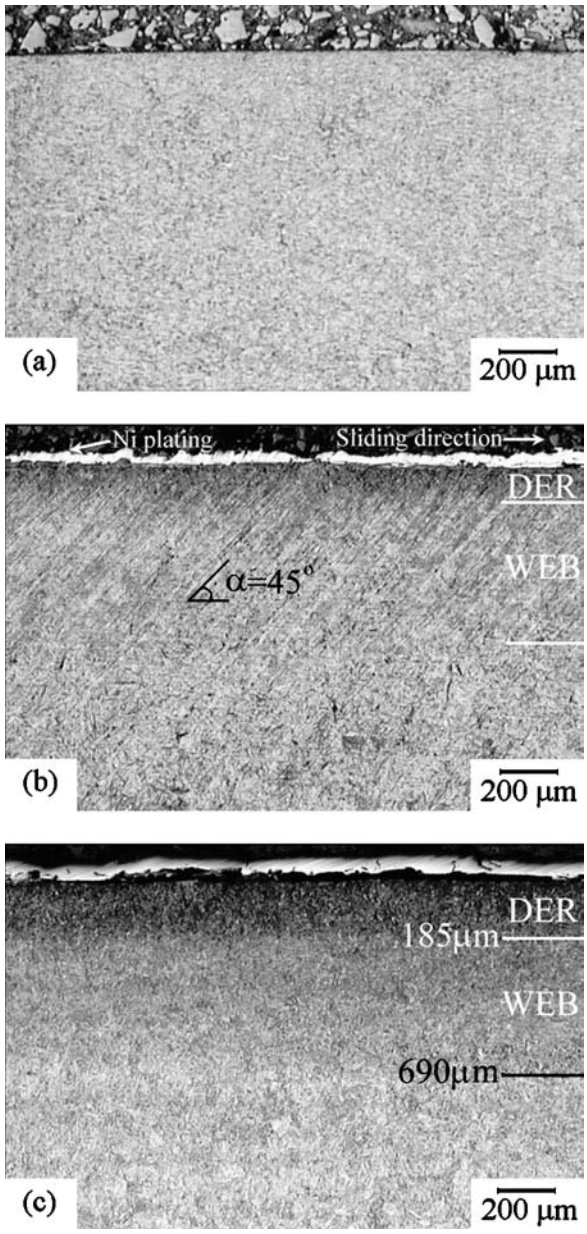

Figure 3 Microstructure before and after test. (a) Longitudinal section before test showing no DER or WEB. (b) DER and WEB in longitudinal section. (c) DER and WEB in transverse section. Experiment 1; Etch: nital.

observable as inclined bands in the transverse section from Fig. 3c but as a zone of fine microstructure, lying beneath the DER, slightly darker than the unaffected microstructure.

Fig. 4 shows the microstructure of the specimen tested in experiment 3. The development of WEB is more advanced as compared to the previous case although both specimens were tested for the same number of stress cycles. The DER extends to a depth of 165 μm and WEB to a depth of 890 μm. Since in experiment 3 the contact pressure and the temperature were higher it can be assumed that higher loads and temperatures are favourable to the martensite decay phenomenon. The examination of the transverse section reveals two sets of WEB having opposite orientations and inclined relative to the surface plane at $\alpha_1 = 55^\circ$ and $\alpha_2 = 38^\circ$, respectively.

The two sets of WEB suggest that the transformation is dependent on the Hertzian stress conditions and the

TABLE III The correlation between the depth of maximum shear stress and the centre of the transformed region

Exp.	Depth of maximum shear stress z (μm)	Centre of the transformed region (DER + WEB) (μm)
1	336.5	345
2	425.5	410
3	430	445

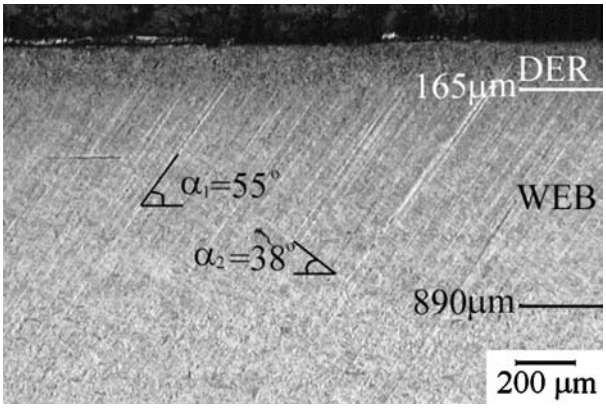

Figure 4 DER and WEB. Transverse section. Experiment 3; Etch: nital.

values of the angles, α_1 and α_2, suggest that the texture develops in the direction of the principal shear stress. Moreover, the transformed region (DER + WEB) is centred on a depth that corresponds to the depth of maximum shear stress determined by Hertzian elastic contact theory [39]. Table III lists the depth of maximum shear stress, z, and the centre of the region with decayed martensite (the half-width of the region DER + WEB) for the specimens tested in experiments 1, 2 and 3.

3.1. Dark etching regions

The SEM images from Fig. 5 were taken from a region at about 20 μm below the surface of the sample tested in experiment 2. The micrograph from Fig. 5a shows a circular distribution of the dark etching phase grains. The diameter of the region is in the range of the diameter of the prior austenite grains, which suggests that the DER phase initiates at the prior austenite grain boundaries. The grains grow and break down the martensite needles until the entire martensitic microstructure, within the prior austenite grain, is transformed (see Fig. 5b).

Fig. 6a shows the microstructure of an untested sample. The prior austenite grain boundary (arrowed) is intact and, numerous, small, spherical carbides can be seen within the martensite needles. In Fig. 6b, which is a longitudinal section taken from specimen 2, the DER appear to break down the prior austenite grain boundary structure and the number of carbide precipitates is reduced. The coarse carbides (arrowed) appear at the boundaries between the initial martensite and the newly formed DER grains. The coarsening of carbides, suggests that temperature plays a significant role in the development of the martensite decay products by facilitating the diffusion of carbon.

Fig. 7 shows the microstructure of the specimen tested in experiment 3 in the region near the surface.

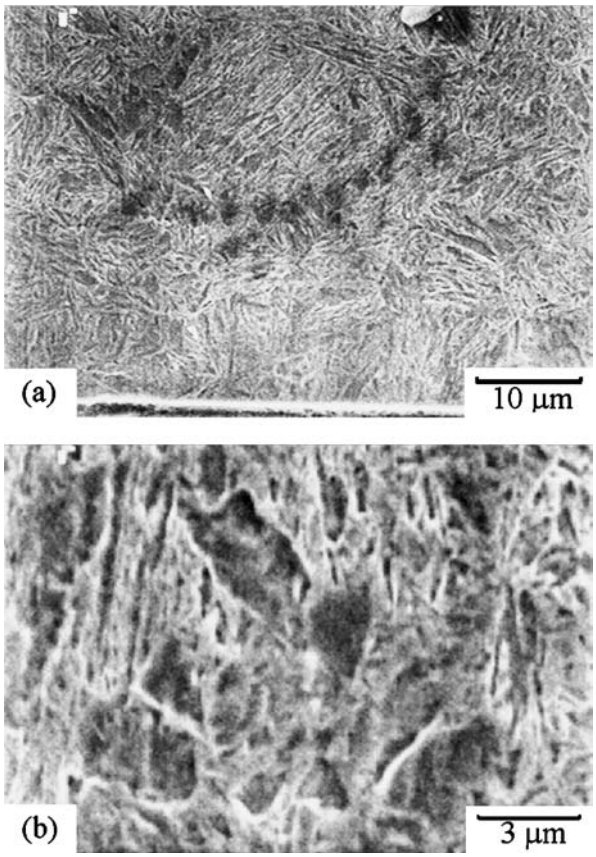

Figure 5 Nucleation of DER. SEM images. (a) DER grains at the prior austenite grain boundary. (b) Higher magnification of DER. Experiment 2; Etch: nital.

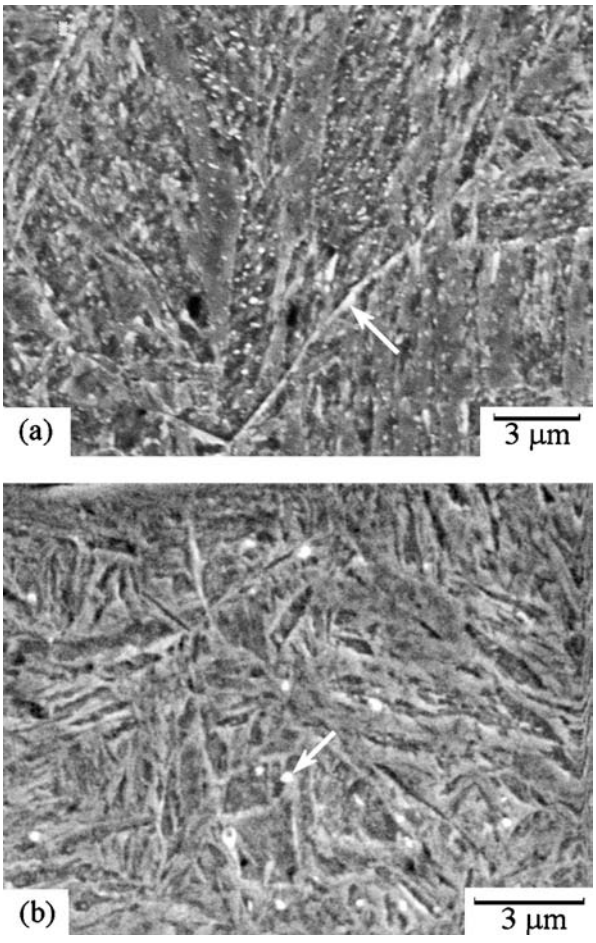

Figure 6 Carbide precipitates. SEM images. (a) Untested specimen, (b) Experiment 2, Etch: nital.

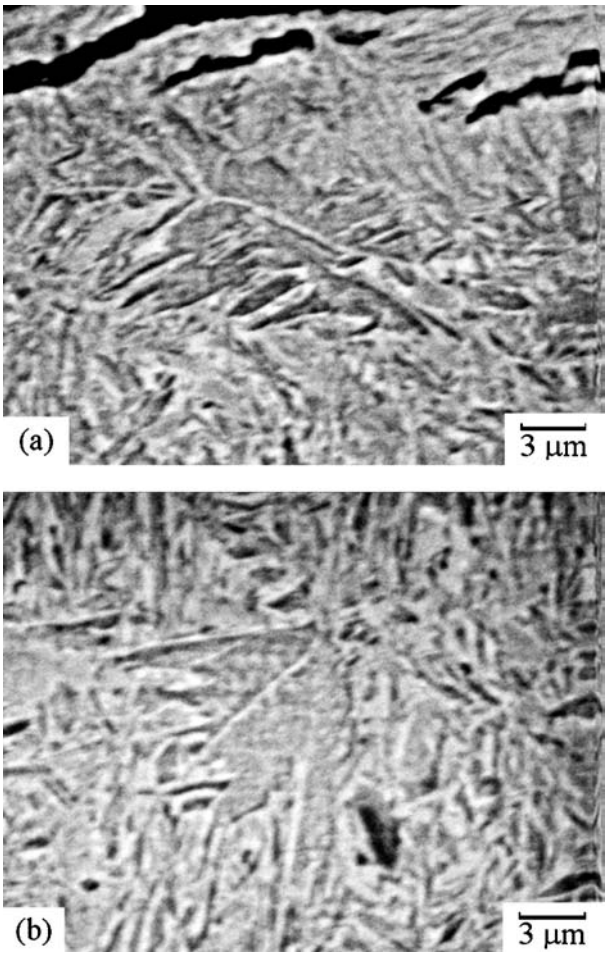

Figure 7 DER initiation at the prior austenite grain boundary. SEM images. Experiment 3. Etch: nital.

The features shown resemble butterflies and they have almost perfect symmetrical wings. No observable inclusions or carbides are associated with these entities. Their shape can vary but the wings appear to develop symmetrically to a central axis. Since non-metallic inclusions or carbide particles cannot be observed within these features but the wings develop symmetrically to a central axis it is suggested that the axis of symmetry is the prior austenite grain boundary and the wings represent zones of DER. The axis of symmetry is not related to the direction of sliding. Figs 9a and b show two different regions of the same specimen and the presumed butterflies have opposite orientations. Taking these observations into account and considering that the hardness value determined for the wings coincides with the hardness of DER (see Section 3.4) it is suggested that the wings are grains of dark etching phase.

3.2. White etching bands

The micrograph from Fig. 8a is a higher magnification of the WEB region shown in Fig. 3b. The martensitic structure is completely replaced by white etching bands of few microns width, separated by larger zones of about 10 μm. The line marked with the letter B is a polishing artefact. Very thin bands (in A), almost perpendicular to the WEB and crossing over them are believed to be the second set of WEB. Fig. 8b

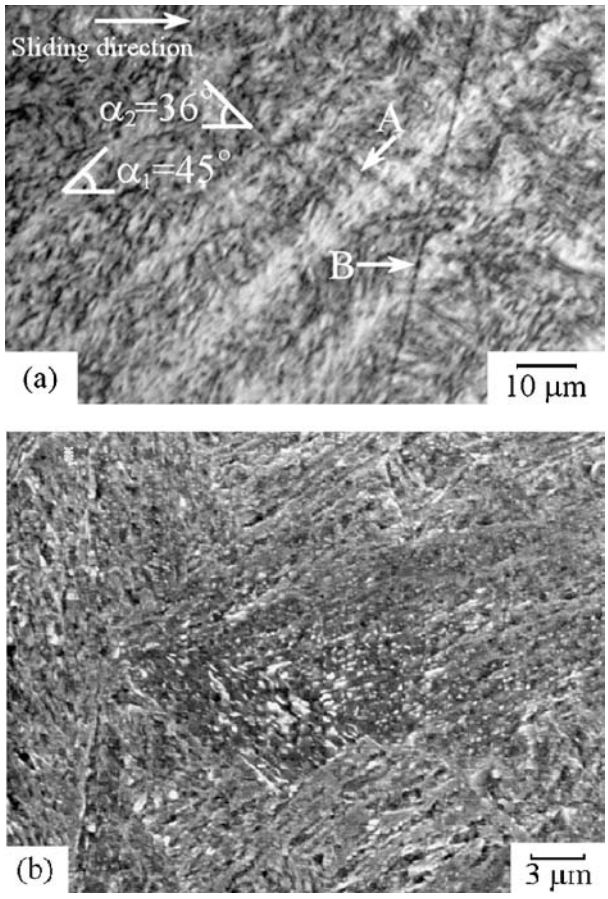

Figure 8 (a) Higher magnification of the WEB shown in Fig 2c. (b) Space between WEB. SEM image. Experiment 1; Etch: picral.

depicts a higher magnification of the space between the white etching bands. The microstructure is abundant in carbide precipitates, which explain the high hardness recorded by nanoindentation in this region (see Section 3.4).

3.3. Plastic deformation region

The regions very close to the surface, below asperities are subjected to severe plastic deformation. It is suggested that the accumulated plastic deformation leads to the formation of the layer marked PDR in Fig. 9.

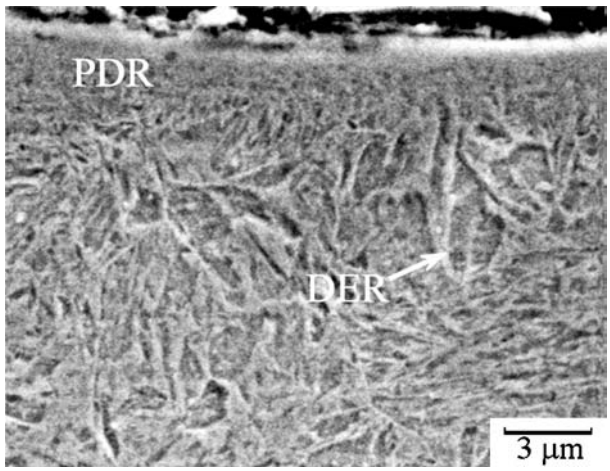

Figure 9 DER grains at the PDR boundary. SEM image. Experiment 1. Longitudinal lay. Longitudinal section. Etch: nital.

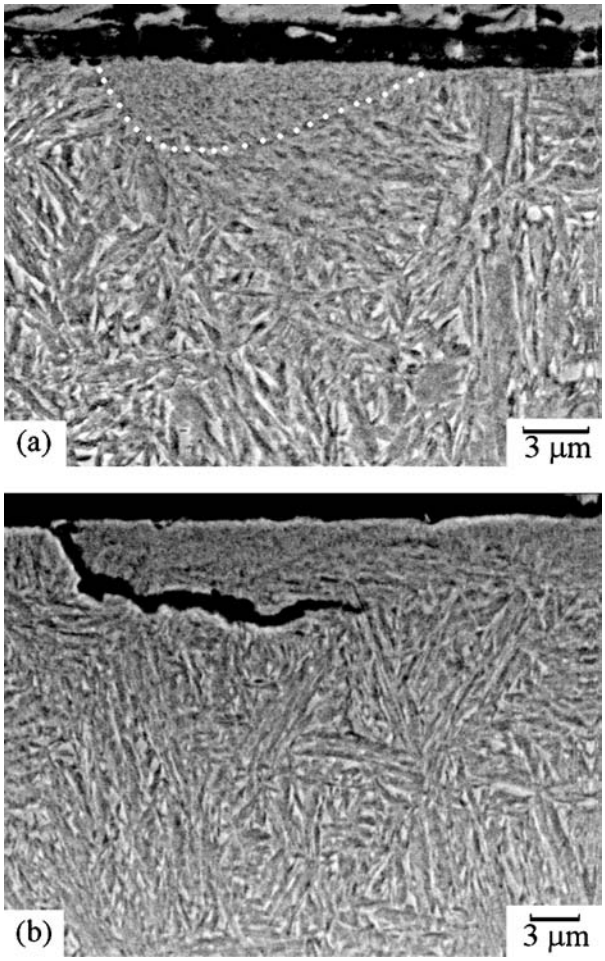

Figure 10 SEM images showing (a) semi-circular PDR and (b) crack propagation at the PDR boundary. Experiment 1, transverse section; longitudinal lay. Etch: nital.

This microstructural feature will be referred in this work as the plastic deformation region (PDR). The PDR exhibits an apparently non-martensitic microstructure judging by the absence of needles. Big DER grains can be seen in Fig. 9 at the boundary of the PDR. The sample shown in Fig. 9 was taken in longitudinal direction (i.e., parallel to the surface lay). In transverse section (i.e., perpendicular to the surface lay) PDR appear as semi-circular zones, usually less than 10 μm diameter (see the region marked by dots in Fig. 10a).

The shape and the size of the PDR zones suggest they are formed due to the stress localisation induced by asperity contact. The PDR shown in Fig. 9 is much longer than that in Fig. 10a because the entire region beneath the grinding mark was plastically deformed.

The metallographic examination indicates that the boundaries of these regions are preferential sites for microcrack initiation and propagation (see Fig. 10b). The depth to which the PDR extends coincides with the depth of the micropitting cracks. It can be assumed that the critical region where the cracks initiate and propagate is the boundary of the PDR. PDR develop as a semi-circular zone beneath an asperity and the crack initiates at the surface, at the intersection point between the surface and the PDR boundary and propagates along the boundary.

TABLE IV Hardness of different phases present in steel

Phase	Hardness, H (GPa)
Martensite	8 ± 0.7
DER	12.3 ± 0.5
WEB	11.6 ± 0.8
Space between WEB	20.3 ± 1.8
DER wing	12.5 ± 0.4
PDR	13.7 ± 0.6

3.4. Hardness measurement

The hardness of different phases found in fatigued specimens are given in Table IV. It can be seen that the WEB are slightly harder than the original martensite but the space between the bands is much harder due to intense carbide precipitation in these regions (see Fig. 8). The hardness of the PDR suggests that a work hardening process takes place in the regions near the surface. The hardness of the DER wings shown in Fig. 7 is identical to the hardness of the DER. This observation together with the fact that the wings are not associated with non-metallic inclusions or carbides and that they develop symmetrically to an axis which has arbitrary orientation relative to the sliding direction suggests that they are regions of DER formed at the prior austenite grain boundary.

3.5. Micropitting mechanism

Based on the findings presented above the following micropitting mechanism is suggested. When an asperity collides with another one from the mating surface it deforms plastically in the direction of sliding as suggested in Fig. 11a. Due to alternating stresses, plastic deformation extends in the areas beneath asperity and the dislocation density increases. The change in dislocation structure causes work hardening. At the same time, temperature is high enough to activate the diffusion of carbon. As a result, within the boundary of the PDR recrystallisation occurs. The newly formed structure is the DER. The dislocations pile up against this boundary and form a slip band by the intrusion/extrusion mechanism. As cycling continues, dislocations accumulate in the slip band and a crack is initiated. Once initiated the crack starts to propagate along the boundary where the DER exhibits a lower hardness.

The decay of martensite progresses towards the bulk as cycling continues. The surface initiated crack continues to propagate along the PDR boundary until it reaches the surface leading to the formation of a micropit (see Fig. 11b). The DER that forms at the prior austenite grain boundary provides regions where a crack is more likely to propagate. As a result crack branching may occur until a complex network of cracks forms below the surface. Every time one of these branches reaches the surface the volume of the material removed from the surface increases and hence the micropit will widen and deepen. It is also possible that two cracks generated below two neighbouring asperities intersect each other resulting in a wider and deeper micropit.

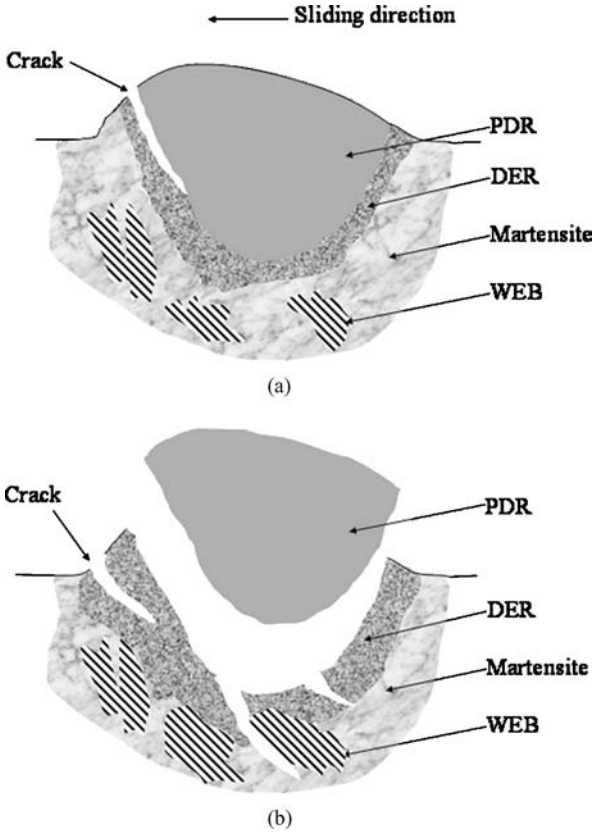

Figure 11 Schematic representation of micropitting initiation (a) and micropitting propagation (b).

4. Discussion

Results generated in this study confirm that the hardness of DER is greater than the original martensite as previously observed [19]. However, the amount of retained austenite in the samples tested here is quite low (∼7%) and low nanoindentation hardness values (H ∼ 3.5 GPa) are observed if regions of retained austenite are indented. Previous reports of softening in the DER [2, 10, 17] are probably related to this.

Previous researchers reported that DER and butterfly wings have the same microstructure [12] but the butterfly's wing hardness is higher [4, 24] than the martensite matrix while the DER hardness is lower [2, 10, 17]. This contradiction is caused by the method used to measure hardness. The microhardness testing (Vickers, Knoop, etc.) gives an average value of the hardness of DER mixture (DER-ferrite, martensite and retained austenite). The use of the nanoindentation technique has revealed that DER-ferrite and butterfly wings have similar hardness ($H \sim 12.5$ GPa). Moreover, it was shown that butterfly-like features were formed at the prior austenite grain boundary, the preferred location for DER initiation.

Up to the present study no data existed on the hardness of the WEB. The results confirm the existing theory [5, 13, 17] according to which carbon from the bands migrates in their vicinity. This explains the high hardness recorded in the space between the bands. The comparison between axial and circumferential grinding of samples tested here has highlighted the importance of preparing samples which closely match those used in the application if failure mechanisms are to be understood. Longitudinal grinding produces asperities elongated in the sliding direction and the PDR is similarly extended. Cracks which propagate parallel to the surface, at the PDR/DER boundary, will be produced in micropitting tests (such cracks were observed). Transverse grinding leads to asperities extended perpendicular to the sliding direction and semicircular crack paths around the PDR beneath the asperity. Micropitting is much more likely in such cases.

Previous workers have tried to explain the micropitting phenomenon in terms of slip line field theory [32] or lubricant pressure effects [31]. However, this study has demonstrated a microstructural aspect to the crack nucleation and propagation process. Since propagation occurs at the PDR/DER boundary and this depends on the size and shape of asperities and the location of prior austenite grain boundaries control of these factors will enable micropitting to be reduced.

It has been stated [25] that fatigue cracks tend to propagate along WEB. However, as indicated in Figs 3 and 4 WEB do not extend in the region where the micropitting cracks are seen (up to 20 μm deep), therefore it can be concluded that WEB are not responsible for micropitting. It should be mentioned that the orientation of WEB observed here is different than the WEB orientation in bearings where the second set of bands is always oriented in the same direction as the first set and WEB at 45° to the surface were never observed [40]. These differences are probably due to the slip component in rolling/sliding contacts. With a few exceptions [41] the contact traction was not considered in analysis of WEB orientation.

The micropitting mechanism suggested here can be applied to gears since PDR and DER develop similarly [29].

5. Conclusions

The metallographic investigation of the contact fatigued discs has revealed a number of microstructural features that are not present in untested specimens. Near the surface, zones that exhibit high hardness ($H = 13.7 \pm 0.6$ GPa) were found. These regions (PDR) appear as semi-circular zones, usually less than 10 μm diameter. At higher depths dark etching regions (DER) and white etching bands (WEB) were observed. The dark etching regions initiate at the prior austenite grain boundary. The white etching bands are slightly harder ($H = 11.6 \pm 0.8$ GPa) than the original martensite ($H = 8 \pm 0.7$ GPa) but the space between the bands is much harder ($H = 20.3 \pm 1.8$ GPa) due to intense carbide precipitation in these regions. It has been found that the boundaries of the PDR are preferential sites for microcrack initiation and propagation.

Acknowledgments

The authors are grateful to the Design Unit—Newcastle University for collaboration and financial support during this project.

References

1. A. B. JONES, *Proc. ASTM* **46** (1946) 1.
2. J. J. BUSH, W. L. GRUBE and G. H. ROBINSON, *Trans. ASM* **54** (1961) 390.
3. A. J. GENTILE, E. F. JORDAN and A. D. MARTIN, *Trans. Met. Soc. AIME* **233** (1965) 1085.
4. W. E. LITTMAN and R. L. WIDNER, *Trans. ASME J. Basic Eng.* **Sep.** (1966) 624.
5. J. A. MARTIN, S. F. BORGESE and A. D. EBERHARDT, *Trans. ASME J. Basic Eng.* (1966) Sep. 555.
6. J. L. O'BRIEN and A. H. KING *J. Iron & Steel Inst.* **Jan.** (1966) 55.
7. *Idem.*, *Trans. ASME J. Basic Eng.* **Sep.** (1966) 568.
8. J. BUCHWALD and R. W. HECKEL *Trans. ASM* **61** (1968) 750.
9. H. SWAHN, L. HELLNER, C. G. ANDERSSON, B. ZETTERLUND and O. VINGSBO, *Scandinavian J. Met.* **4** (1975) 263.
10. H. SWAHN, P. C. BECKER and O. VINGSBO, *Met. Trans.* **7A** (1976) 1099.
11. *Idem.*, *Met. Sci.* **Jan.** (1976) 35.
12. P. C. BECKER, H. SWAHN and O. VINGSBO, *Mecanique, Materiaux, Electricité* (1976) **320/321** Aug/Sep, 8.
13. R. ÖSTERLUND and O. VINGSBO *Met. Trans.* **11A** (1980) 701.
14. A. P. VOSKAMP, R. ÖSTERLUND, P. C. BECKER and O. VINGSBO, *Met. Tech.* **Jan.** (1980) 14.
15. E. LINDHAL and R. ÖSTERLUND, *Ultramicroscopy* **9** (1982) 355.
16. B. Y. CHOI and G. W. BAHNG, *Mat. Sci. & Tech.* **14** (1985) 816.
17. A. P. VOSKAMP, *ASME J. Tribol.* **107** (1985) 359.
18. V. BHARGAVA, G. T. HAHN and C. A. RUBIN, *Met. Trans.* **21A** (1990) 1921.
19. A. MUROGA and H. SAKA, *Scr. Met. Mat.* **33(1)** (1995) 151.
20. A. P. VOSKAMP and E. J. MITTEMEIJER, *Met. & Mat. Trans.* **27(A)** (1996) 3445.
21. A. P. VOSKAMP and E. J. MITTEMEIJER, *Z. Metallkd.* **88(4)** (1997) 310.
22. A. P. VOSKAMP, *ASTM STP* **1327** (1998) 152.
23. H. STYRI, *Proc. ASTM* **51** (1951) 682.
24. R. ÖSTERLUND, O. VINGSBO, L. VINCENT and P. GUIRALDENQ, *Scandinavian J. Met.* **11** (1982) 23.
25. A. P. VOSKAMP and G. E. HOLLOX, *ASTM STP* **987** (1988) 102.
26. J. BESWICK, A. VOSKAMP, J. SANDEN, M. VERBURGH and S. HORTON, *ibid.* **1195** (1993) 222.
27. M. R. HOEPRICH, in "Proceedings of the 12th International Colloquium: Tribology 2000-Plus," edited by W.J. Bartz (Technische Akademie Esslingen, 2000) vol. 3, p. 2023.
28. H. WINTER, G. KNAUER and J. J. GAMEL *Gear Technol.* Sep./Oct. (1989) 18.
29. A. OILA, PhD thesis. University of Newcastle, 2003, p. 262.
30. B. A. SHOTTER, in "Performance and testing of gear oils and transmission fluids - Proceedings of the International Symposium," edited by R. Tourret and E.P. Wright (The Institute of Petroleum, London, 1980) p. 451.
31. A. F. BOWER, *Trans. ASME J. Tribol.* **110** (1988) 704.
32. A. V. OLVER, in "Proceedings of the 10th Leeds—Lyon Symposium on Tribology," 1983.
33. A. V. OLVER, H. A. SPIKES, A. F. BOWER and K. L. JOHNSON, *Wear* **107** (1986) 151.
34. M. N. WEBSTER and C. J. J. NORBART, *Tribol. Trans.* **38**(4) (1995) 883.
35. L. FLAMAND, D. BERTHE and M. GODET, *Trans. ASME—J. Mech. Des.* **103** (1981) 204.
36. G. F. VANDER VOORT, "Metallography, Principles and Practice," (McGraw-Hill, New York, 1984) p. 752.
37. W. C. OLIVER and G. M. PHARR, *J. Mater. Res.* **7**(6) (1992) 1564.
38. A. OILA and S. J. BULL, *Z. Metallkd.* **94**(7) (2003) 793.
39. K. L. JOHNSON, "Contact Mechanics," (Cambridge University Press, Cambridge, 1987) p. 452.
40. I. A. POLONSKY and L. M. KEER, *J. Mech. Phys. Solids* **4** (1995) 637.
41. K. L. Johnson, Research Report CUED/C-MECH/TR42.

Received 2 June 2004
and accepted 3 February 2005